Spark Plasma Sintering Assisted Carbon Conversion from Various Modifications to Diamond

F. Zhang, C. Mihoc, E. Burkel
Institute of Physics, University of Rostock, August Bebel Str. 55, Rostock 18055, Germany

Keywords: Carbon nanotubes, Phase transformation, Diamond synthesis, Spark plasma sintering.

Abstract

The spark plasma sintering (SPS) is a novel sintering technique for fast sintering of nanostructured ceramics and metals and nanocomposites. It was found that diamond even could be converted from carbon nanotubes (CNTs) by using the SPS. It was proposed that the spark plasmas play a key role to provide most of the energy required in this diamond transition. In this study, the SPS assisted diamond conversion was investigated by varying different carbon modifications: CNTs, C60 and graphite. The results show that diamond could be converted from CNTs and C60 without catalysts being involved by the SPS. However, there is no diamond formation in the graphite sample without catalysts during the SPS. Their phase transitional mechanisms from CNTs and C60 to diamond under such novel sintering technique were investigated. Their transitional mechanisms indicated the presence of plasmas during the SPS process.

Introduction

Spark plasma sintering (SPS), also defined as field assisted sintering technique (FAST) or pulsed electric current sintering (PECS), is a electric field assisted sintering process utilizing ON-OFF DC pulse energizing [1]. During the SPS treatment, pulsed DC current directly passes through the graphite die, as well as the powder compact, in case of conductive samples. During study of the thermal stability of multi-walled carbon nanotubes (MWCNTs) under various SPS conditions, it was found that under SPS conditions of 1500 ^{o}C at very low pressure (80 MPa) carbon nanotubes are unstable and transform to diamonds without any catalysts being involved [2-4]. It is proposed that the spark plasmas play a key role to provide most of the energy required in this diamond transition [2, 3]. These studies indicate that the SPS has a potential to be used as an alternative method for diamond generation, and it also provide an indirect way to validate the existence of the plasmas during the SPS. However, this point still needs further investigations due to the still on-going argument about whether the spark plasmas actually occur during the SPS process. In this study, the SPS assisted diamond conversion was investigated by varying different carbon modifications: CNTs, C60 and graphite. The pure CNTs, C60 and graphite powders were processed by using the SPS. Their phase constitutions before and after sintering were investigated by using synchrotron radiation. Their phase transitional mechanisms under such novel sintering technique were investigated thermodynamically.

Experimental

The MWCNTs (10-20 nm) with purity above 95% were obtained from Shenzhen Nanotech Port, Ltd., China. The C60 with purity of 99.5% was obtained from SES Research, Huston, USA. The graphite powders with purity of 99.0% were purchased from Alfa Aesar, Germany. The carbon powders were pressed into a graphite die for SPS treatment to form disk-shaped samples of 20 mm diameter and 5 mm thickness. The SPS experiments were conducted using a Model HPD-25/1 FCT spark plasma sintering system (FCT systeme GmbH, Rauenstein, Germany), under an axial pressure of 80 MPa in a vacuum condition. A heating rate of 100 K/min was adopted, and the sintering process lasted typically 20 min. The applied direct current for SPS was about 1000 A, with a pulse duration of 12 ms and an interval of 2 ms.

The phase identification of the obtained carbon samples was performed using high-energy X-ray diffraction at HASYLAB beamline BW5 (DESY synchrotron facility, Hamburg). The samples were illuminated for 120 seconds by a well collimated 1x1 mm^2 monochromatic beam with the wavelength of 0.15339 Å (80.828 keV). XRD patterns were collected in a transmission mode using a two-dimensional detector (MAR345 image plate) positioned symmetrically with respect to the beam. A LaB6 reference material was used to calibrate the sample-to-detector distance and the tilt of the imaging plate relative to the beam path. The obtained XRD data were integrated by using the FIT2D program.

Results

The pure MWCNTs were spark plasma sintered at 1500 ^oC under pressure of 80 MPa for holding time of 20 min. Figure 1 shows the synchrotron radiation diffraction patterns of the raw MWCNTs and the spark plasma sintered MWCNTs at 1500 ^oC, 80 MPa for 20 min. The raw MWNCTs show a main diffraction peak at 3.43 Å corresponding to the CNTs (002) plane spacing and a weak peak at 2.10 Å corresponding to the CNTs (100) plane spacing. After SPS processing, the MWCNTs diffraction peaks still present in the sintered MWCNTs compacts, but the cubic diamond peaks were detected in the sample those centered at 2.05, 1.23 and 1.06 Å corresponding to the cubic diamond (111), (220) and (311) plane spacing, respectively.

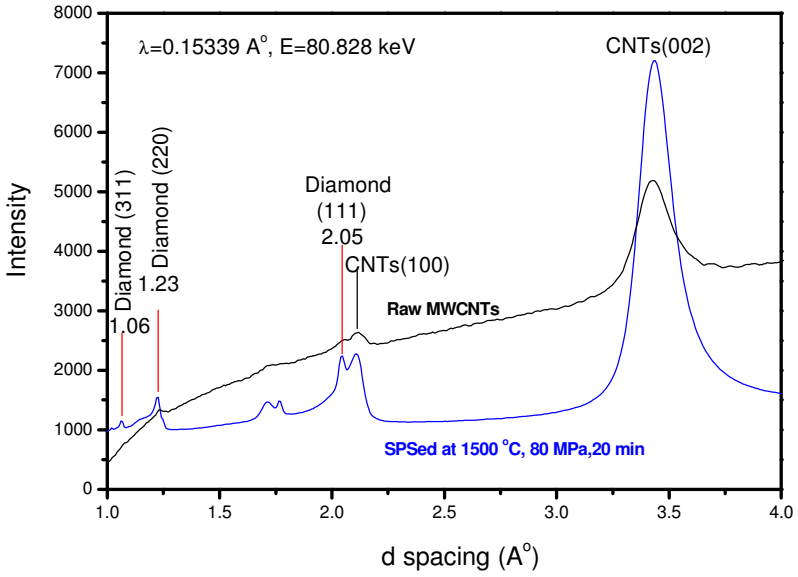

Figure 1 Synchrotron radiation diffraction patterns of the raw MWCNTs and the spark plasma sintered MWCNTs at 1500 ^{o}C, 80 MPa for 20 min.

Figure 2 shows the synchrotron radiation diffraction patterns of the raw C60 and the spark plasma sintered C60 at 1500 ^{o}C, 80 MPa for 20 min. The raw C60 exhibits diffraction peaks at d spacing of 5.01, 4.28, 4.11, 3.18, 2.9, 2.74 Å belonging to C60 (110), (112), (004), (114), (300), (006) planes (PDF# 47-0787), respectively. The C60 after spark plasma sintering at 1500 ^{o}C under 80 MPa for 20 min shows the cubic diamond diffraction peaks at d spacing of 2.06 and 1.23 Å. The C60 diffraction peaks disappeared indicating the C60 has transformed into diamond phases after SPS.

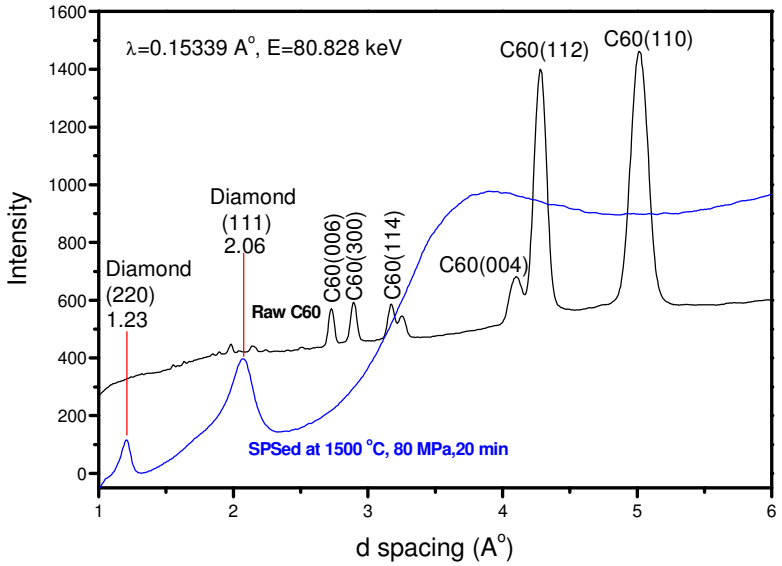

Figure 2 Synchrotron radiation diffraction patterns of the raw C60 and the spark plasma sintered C60 at 1500 ^{o}C, 80 MPa for 20 min.

Figure 3 shows the synchrotron radiation diffraction patterns of the raw graphite and the spark plasma sintered graphite at 1500 ^{o}C, 80 MPa for 20 min. The raw graphite sample presents Graphite-3R and Graphite-2H diffraction peaks those are centered at 3.348 Å [G-3R(003)], 1.674 Å [G-3R(006)], 1.228 Å [G-3R(110)] (PDF#26-1079), and 2.138 Å [G-2H(100)] , 2.039 Å [G-2H(101)], 1.16 Å [G-2H(112)] (PDF#41-1487). However, the graphite samples after the SPS exhibit the identical diffraction results with the raw graphite. There is no diamond conversion from pure graphite during the SPS.

Discussion

Synchrotron radiation was used to identify the diamond phase in the carbon samples after spark plasma sintering. The synchrotron radiation generated by the acceleration of ultrarelativistic (moving near the speed of light) charged particles through magnetic fields are extremely intense, highly collimated and highly polarised [5]. It can penetrate all the spark plasmas sintered carbon pellets, while the conventional X-ray diffraction using CuKα radiation only can detect the surface of the sample. By using the synchrotron radiation, the cubic diamond

phases were identified in the spark plasma sintered MWCNTs and C60 samples. The standard d spacing of the cubic diamond (111), (220) and (311) planes are centered at 2.059 Å, 1.261 Å and 1.075 Å (PDF# 65-0537). The diffraction peaks of the synthesized diamond from MWCNTs and C60 are very close to the standard diamond diffraction data. The peaks shifts are due to the existence of residual stress in the synthesized diamonds from MWCNTs and C60 by using the SPS. The residual stress of the diamond is because of the stress that remains after the original cause of the stresses (uniaxial forces, heat gradient) has been removed. There are no C60 diffraction peaks in the spark plasma sintered C60 sample, there are strong unreacted MWCNTs peaks in the spark plasma sintered MWCNTs sample, and there are no diamond phases in the spark plasma sintered graphite sample. It is indicated that the energy status of C60 is higher than the MWCNTs, and MWCNTs is higher than the graphite. The graphite is the most stable carbon among the C60, MWCNTs, and graphite allotropes.

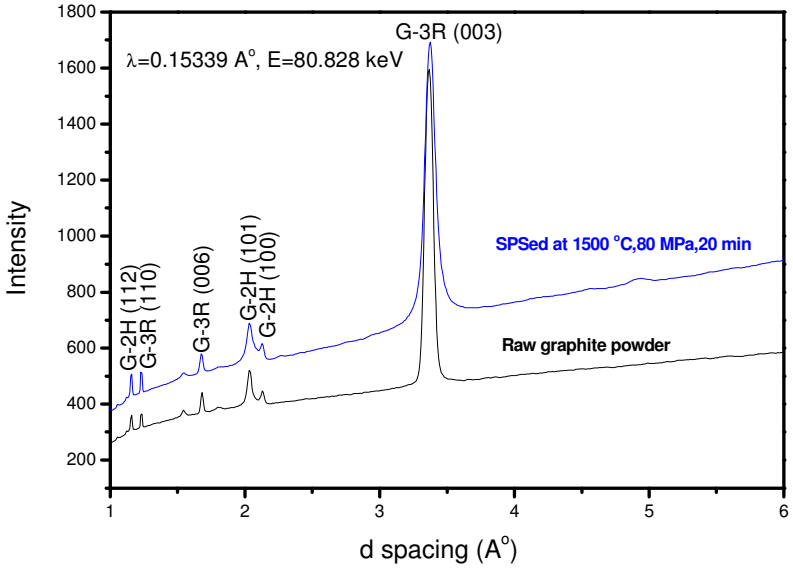

Figure 3 Synchrotron radiation diffraction patterns of the raw graphite and the spark plasma sintered graphite at 1500 ^{o}C, 80 MPa for 20 min.

We found that the multi-walled carbon nanotubes and C60 are dynamically stable at this 1500 ^{o}C temperature under 80 MPa in a non-oxygen atmosphere during the conventional sintering. Thus, such a significant difference in the products must be due to the special sintering principle of SPS. It is a field activated sintering technique based on an electric spark discharge phenomenon, i.e. a high energy and low voltage spark pulse current momentarily generating sparking plasma which causes localized high temperatures. We believe that the spark plasma contributes to the diamond conversion from carbon nanotubes and C60 during the SPS. Despite the on-going argument about whether the spark plasmas actually occur during the SPS process, our present study, generating diamond under such a low pressure, suggests that such sparking plasmas indeed took place during SPS, and they dramatically reduced the pressures required for diamond formation from the GPa to the MPa level. So, we take plasma into consideration in the thermodynamic analysis.

The total energy for the diamond formation:

$$Q = \Delta H_T + Q_P + \Delta H_M$$

Where Q —Total Energy;

ΔH_T—Energy of temperature;

Qp—Energy of pressure;

ΔH_M—Energy of plasma;

The enthalpy of plasma:

$$H = H_K + H_B + H_D + H_I$$

Where H— Plasma contribution;

H_E— kinetic contribution;

H_K— excitation contribution;

H_D—dissolution contribution ;

H_I— electrolytic contribution.

$$\left(\frac{\partial \Delta G}{\partial T}\right)_p = -\Delta S$$

$$\Delta G(T) - \Delta G(T^0) = -\int_{T^0}^{T} \Delta S dT = \Delta S(T^0 - T)$$

Where T—Temperature ;

T_0—Starting temperature ;

ΔG—Difference of mol free energy ;

ΔS—Difference of mol entropy.

Only if $\Delta G(T)<0$, CNTs and C60 can be transformed into diamond. So, we can get a function:

$$T > T^0 + \frac{\Delta G(T^0)}{\Delta S}$$

The pressure used in this study was 80 MPa. The effect of the plasma in the SPS has increased the entropy of the whole SPS system resulted a lower sintering temperature (1500 ^oC) for the diamond formation. Without plasma effect, it will need 8000-10000 ^oC at pressure of 80 MPa. Therefore, the hydrostatic HPHT technique need several GPa super-high pressure for the diamond formation. Since the SPS only needs MPa level pressure, the plasma plays the key role for the diamond formation, increasing the entropy of the SPS system.

Conclusions

Diamond has been converted from pure CNTs and C60 without involving catalysts by the SPS technique. There was no notice of diamond formation in the case of pure graphite sample processed by SPS, when no catalysts are used. The energy status of C60 is higher than the MWCNTs, and MWCNTs is higher than the graphite. The graphite is the most stable carbon among the C60, MWCNTs, and graphite allotropes. The thermodynamic analysis on the phase transitional mechanisms from CNTs and C60 to diamond indicated the presence of plasmas during the SPS process. The plasma in the SPS has increased the entropy of the whole SPS system resulted milder conditions for the diamond formation.

Acknowledgments

This research is supported by the DFG-Deutschen Forschungsgemeinschaft (German Research Foundation) with grant No. BU 547/10-1, and DESY HASYLAB Project with grant No. II-20090264.

References

[1] Z. A. Munir, U. Anselmi-Tamburini, The effect of electric field and pressure on the synthesis and consolidation of materials: A review of the spark plasma sintering method, *J Mater. Sci.*, Vol 41, 2006, p 763–777.
[2] F. Zhang, J. Shen, J. Sun, Y. Q. Zhu, G. Wang and G. McCartney, Conversion of carbon nanotubes to diamond by a spark plasma sintering, *Carbon*, Vol 43, 2005, p 1254-1258.
[3] J. Shen, F. M. Zhang, J. F. Sun, Y. Q. Zhu and G. McCartney. Spark plasma sintering assisted diamond formation from carbon nanotubes at very low pressure, *Nanotechnology*, Vol 17, 2006, p 2187-2191.
[4] F. Zhang, J. Shen, J. Sun, D.G. McCartney, Direct synthesis of diamond from low purity carbon nanotubes, *Carbon*, Vol 44, 2006, p 3136-3138.
[5] E. Burkel, Introduction to X-ray scattering, *J. of Phys.: Cond. Matt*, Vol 13, 2001, p 7477-7498.